Pilot Deployment of the LDSD Parachute via a Supersonic Ballute

Christopher L. Tanner*, Clara O'Farrell†, John C. Gallon‡ Ian G. Clark§

Jet Propulsion Laboratory, California Institute of Technology, Pasadena, CA, 91109, USA

Allen Witkowski¶, Paul Woodruff‖

Pioneer Aerospace Corporation, South Windsor, CT, 06074, USA

The Low Density Supersonic Decelerator (LDSD) Project required the use of a pilot system due to the inability to mortar deploy its main supersonic parachute. A mortar deployed 4.4 m diameter supersonic ram-air ballute was selected as the pilot system for its high drag coefficient and stability relative to candidate supersonic parachutes at the targeted operational Mach number of 3. The ballute underwent a significant development program that included the development of a new liquid methanol-based pre-inflation system to assist the ballute inflation process. Both pneumatic and pyrotechnic mortar tests were conducted to verify orderly rigging deployment, bag strip, inflation aid activation, and proper mortar performance. The ballute was iteratively analyzed between fluid and structural analysis codes to obtain aerodynamic and aerothermodynamic estimates as well as estimates of the ballute's structural integrity and shape. The ballute was successfully flown in June 2014 at a Mach number of 2.73 as part of the first LDSD supersonic flight test and performed beyond expectations. Recovery of the ballute indicated that it did not exceed its structural or thermal capabilities. This flight set a historical precent as it represented the largest ballute to have ever been successfully flown at this Mach number by a NASA entity.

Nomenclature

a_{TV}	acceleration of the test vehicle
C_D	drag force coefficient
Δt_{ls}	time from mortar fire to line stretch
V_0	mortar muzzle velocity
V_{ls}	velocity at line stretch
x_{ls}	distance to line stretch
CFD	Computational Fluid Dynamics
FEA	Finite Element Analysis
FLL	Flight Limit Load
fps	Frames Per Second
IA	Inflation Aid
LDSD	Low Density Supersonic Decelerator

*LDSD Parachute Deployment Device Cognizant Engineer, Member AIAA.
†Data Analyst, Member AIAA.
‡LDSD PDS Cog-E, Member AIAA.
§LDSD Principal Investigator, Member AIAA.
¶Director of Engineering Operations, AIAA Associate Fellow.
‖Ballute Systems Engineer, AIAA Senior Member

PDD	Parachute Deployment Device
SIAD	Supersonic Inflatable Aerodynamic Decelerator
SFDT	Supersonic Flight Dynamics Test
TPS	Thermal Protection System
TV	Test Vehicle
V&V	Verification and Validation

I. Introduction

Due to the presence of a solid rocket motor in the center of the flight test vehicle (TV), the Low Density Supersonic Decelerator (LDSD) supersonic parachute was stowed approximately 1.1 m from the vehicle axis of symmetry (centerline of the vehicle to centerline of the parachute can). This off-centerline position precluded the ability to mortar deploy the 100 kg parachute pack due to the excessive structural requirements of such a mortar and the large tip-off moments imparted to the vehicle in flight. This resulted in the need to extract the parachute from its container via a pilot system, referred to as the Parachute Deployment Device (PDD).

The PDD system consists of a mortar, a supersonic ram-air inflated ballute, and a bridle assembly. A ram-air inflated supersonic ballute was selected over a supersonic pilot parachute for to its higher drag coefficient, greater stability, and more deterministic opening behavior at the relatively high deployment Mach condition. The LDSD supersonic flight TV is shown in Figure 1 with the PDD-related components indicated.

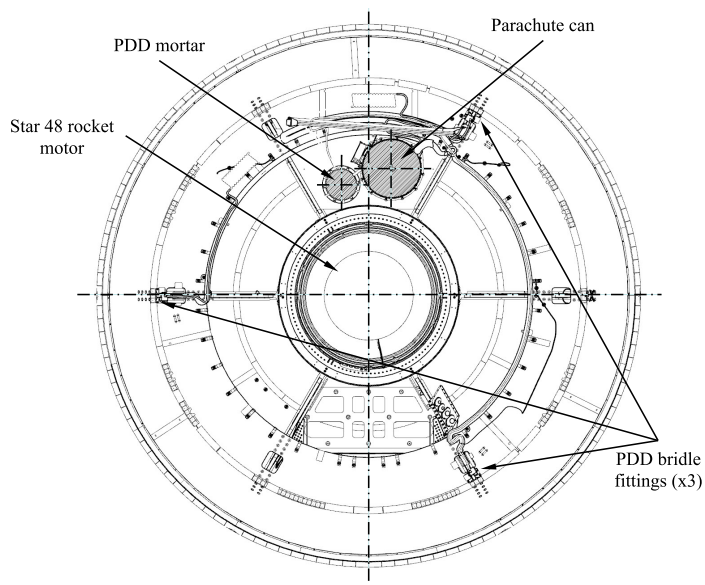

Figure 1: LDSD supersonic TV with PDD components indicated.

At a nominal altitude of 50 km and a Mach number of approximately 2.75, the ballute is ejected from the TV by the mortar and the ballute inflates upon reaching the end of its bridle assembly. The ballute remains attached to the vehicle for five seconds to stabilize and obtain drag performance data, then the bridles are cut away from the vehicle and the ballute extracts the parachute pack for deployment. Even though the ballute is used as a pilot device to extract the parachute, the LDSD project wanted to maintain similarity to the traditional mortar deployment method of all previous Mars flight missions. To accomplish this similarity, the ballute is cut away from the parachute prior to line stretch so that the parachute pack achieves a velocity and deceleration profile similar to a mortar deployment at line stretch. This mortar similarity condition is referred to as "mortar extensibility" and is detailed extensively by Adams.[1] The parachute deployment process is described in greater detail by Gallon et al.[2] This paper presents a general summary of the PDD system, the pre-flight analysis and testing of the system components, and its performance during the first LDSD supersonic test flight in the summer of 2014.

II. Ballute Assembly Overview

A. Ballute Description

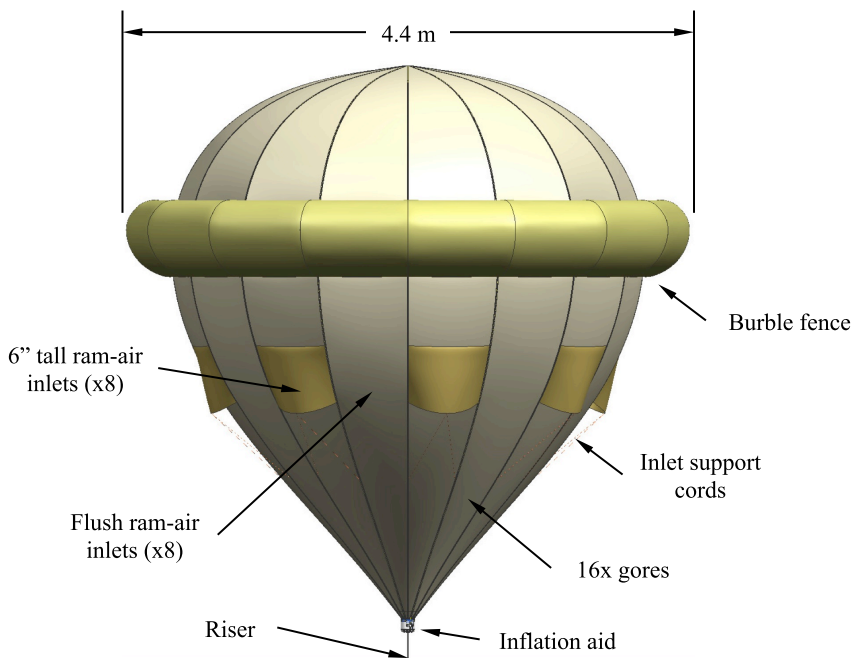

Figure 2: Ballute diagram.

A diagram of the LDSD ballute is shown in Figure 2 highlighting important features and dimensions. The ballute was designed to have a maximum diameter of 4.4 m when fully inflated at its design deployment condition of Mach 3 and flight limit load (FLL) of 1680 lb. The ballute features a 10% burble fence (i.e. the radius of the burble fence is equal to 10% of the maximum radius of the main ballute envelope), which is designed to increase the stability of the ballute by creating a well-defined flow separation point all the way around the ballute, as well as increase drag by increasing the maximum diameter of the device.

The ballute features 16 ram-air inlets in two alternating configurations. All of the inlets are open and functional during inflation in order to quickly ingest a large amount of air and inflate that ballute quickly. Eight inlets are designed with zero fullness and effectively close flush against the surface of the ballute when it is fully inflated. The eight other inlets have sufficient fullness to remain 6 in tall (as measured perpendicular to the local ballute surface) when the ballute is fully inflated to maintain envelope pressure through its operation. The tall inlets have a set of inlet support cords that extend from the top of the inlet in a V-shape to the meridian on either side of the inlet.

The broadcloth consists of a 60x60 plain weave of Kevlar 29 that weighs approximately 4 oz/yd^2 and has a strength of approximately 400 lb/in. The broadcloth is coated on one-side with approximately 1 oz/yd^2 of silicon to achieve near-zero permeability through the material (resulting in a total coated broadcloth weight of approximately 5 oz/yd^2). The meridians consist of 550 lb Kevlar webbing that is 1/2 in wide. The ballute was fabricated in 16 gores with the broadcloth in block orientation. Block construction was selected (over bias construction) in order to avoid diagonal seams across each gore that may have resulted in higher permeability and/or potential weak areas. The ballute was designed and fabricated by the Pioneer Aerospace Corporation and additional information on the ballute design and construction are provided by Woodruff et al.[3]

B. Inflation Aid Description

At the front of the ballute is a gas generator referred to as the Inflation Aid (IA), shown in Figure 3. A collar on the IA captures loops at the end of each of the 16 ballute meridians, creating a load path through the IA to the ballute's primary axial structural members. The purpose of the IA was to inject a burst

of gas into the ballute at bag strip to provide the ballute with some initial pressurization, help orient the ram-air inlets for proper functionality, and create a more deterministic inflation profile. Most off-the-shelf solid propellant-based gas generators (i.e. automotive airbag gas generators) discharged gas too quickly and with too much enthalpy, which would have likely resulted in damage to the ballute upon inflation. Instead, a custom gas generator was developed at JPL that used a mixture of liquid methanol and water to supply the inflation gas. Upon activation, redundant pyrotechnics in the IA eject the aqueous methanol into the ballute. A combination of the sudden pressure drop (ballute deployment occurs at approximately 50 km altitude) and the residual heat in the ballute causes the methanol to rapidly vaporize, subsequently pressurizing the ballute. A methanol-based gas generator was similarly used in the development of ram-air inflated isotensoid decelerators in the 1960's, although a soft bladder was used to contain and disperse the methanol instead of a pyrotechnic device.[4] However, not all ram-air decelerators investigated during this time period used an inflation system. A flight test of a 5.5 m diameter ballute was attempted at a Mach number of 3.15, but resulted in structural failure during inflation due to excessive whipping and slow inflation.[5] It was postulated that the lack of an inflation system may have contributed to the slow inflation and thus the structural damage. This test was sufficient evidence for the LDSD project to require an inflation system on the ballute. Historically, the methanol-based pre-inflation systems tended to perform best when they supplied at least 50% of the ballute internal pressure. As such, the LDSD IA was required to supply at least 50% of the ballute internal pressure in less than 0.5 seconds with a 95% likelihood across all trajectory dispersions. Note that the ballute's internal pressure is a function of the freestream dynamic pressure and Mach number due to its use of ram-air inlets, thus the IA could not target a single pressure value.

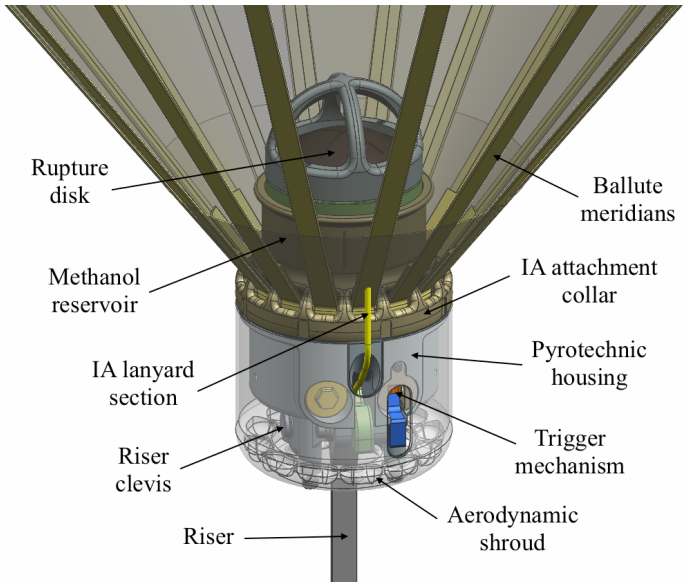

Figure 3: Inflation aid major components and interfaces.

The pyrotechnic charges in the IA were mechanically actuated using a redundant set of lanyards that traveled along opposing sides of the ballute. The lanyards were composed of a combination of Kevlar and Nylon, as shown in Figure 4 – Kevlar for strength near the IA interface and Nylon for compliance to reduce snatch loading into the pyrotechnic firing mechanism. At the IA, the lanyards had a simple knot in the Kevlar section that was seated inside a triggering mechanism such that, when the lanyard was pulled, the lanyards pulled back on the firing pin, then released it at full stroke, igniting the pyrotechnic device. The lanyards were also attached to the ballute just below the burble fence. The burble fence was a relatively large mass concentration in the ballute pack, thus emergence of the burble fence region during bag strip provided a large tension force on the lanyards. The lanyards were fabricated shorter than the distance from the burble fence to the IA to ensure that the lanyards triggered the IA just prior to bag strip completion. A notional diagram of the lanyard functionality during ballute bag strip is shown in Figure 5. For additional information on the inflation aid design and functionality, see the paper by Thompson et al.[6]

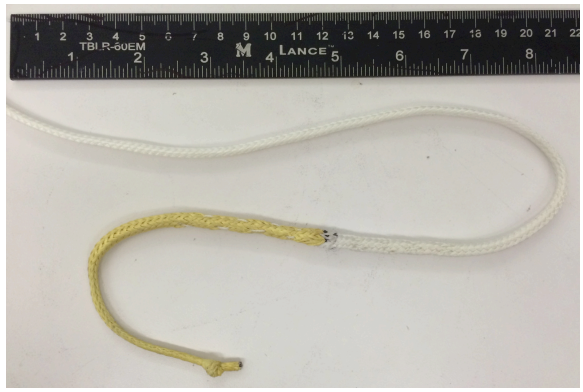

Figure 4: IA lanyard joint between Nylon (white) and Kevlar (yellow) sections.

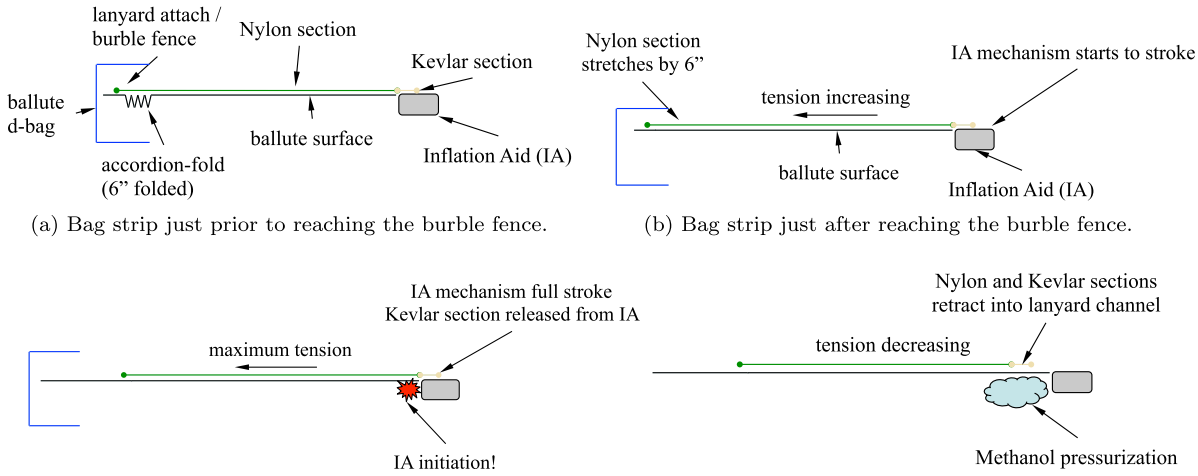

(a) Bag strip just prior to reaching the burble fence.

(b) Bag strip just after reaching the burble fence.

(c) Bag strip after burble fence strip out.

(d) Bag strip complete.

Figure 5: Diagrams notionally showing how the ballute bag strip event causes tension in the IA lanyards and triggers is IA firing mechanism.

C. Bridle Description

The triple bridle assembly consists of a riser and triple bridle. The ballute riser is composed of 12,500 lb Kevlar webbing that is 36.5 m long and connects to the ballute through a clevis in the base of the IA. The riser connects to the triple bridle through a standard parachute metallic link. The triple bridle consists of three 5.5 m long bridle legs composed of 7000 lb Kevlar webbing, each of which connect to the TV through pyrotechnic cutters. The triple bridle also has fourth lazy leg composed of 12,500 lb Kevlar webbing that connects the ballute to the parachute deployment bag for pilot extraction. The ballute nominally flies at a trailing distance of 42 m from the maximum diameter of the TV with the supersonic inflatable aerodynamic decelerator (SIAD) deployed. Figure 6 shows the deployed state of the ballute behind the TV.

Prior to deployment, the bridles were stowed against the aft deck of the vehicle, which means that they would be exposed to the thermal environments generated by the main motor and spin motor plumes. To protect the bridles against these harsh thermal environments, large sections of the bridles were wrapped in S-2 fiberglass and 1 in thick alumina insulation. Additionally, sections of the fiberglass were coated with a silicon RTV to add further protection against potential direct spin motor plume impingement. A similar insulation wrap was placed around the confluence area due to its exposure to the main motor plume as well.

After deployment, the riser and bridles are directly above the main motor, which may still be exhausting residual hot particles and gases. As such, the first 5 m of riser (nearest the confluence) was wrapped in aluminized Kevlar to serve as a protective barrier in case any hot material was exhausted out of the motor after burnout. The upper portions of each of the three bridle legs (nearest the confluence) were similarly

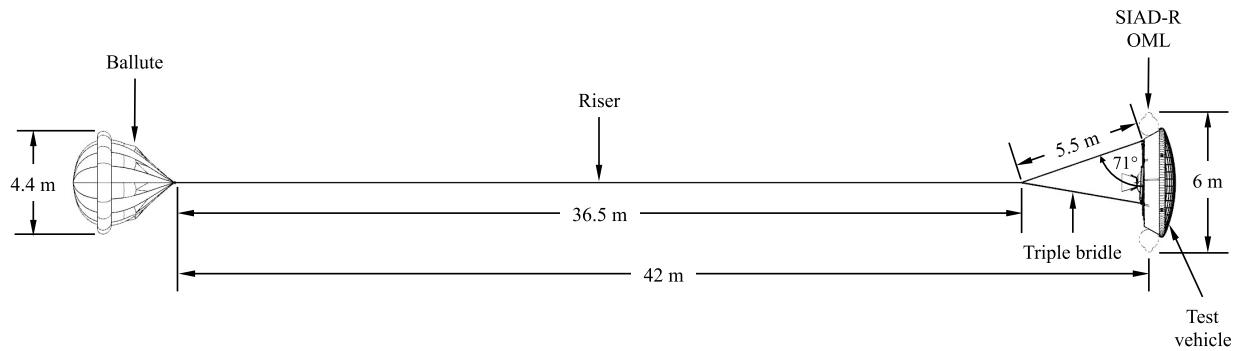

Figure 6: Ballute in its deployed state behind the TV.

wrapped in aluminized Kevlar. These Kevlar barriers also helped protect the integrity of the Kevlar webbing in the event of incidental contact between the brides and the motor nozzle during deployment.

D. Deployment Bag Description

The ballute is pressure packed into its deployment bag to a density of approximately 34 lb/ft^3. The deployment bag features an aluminized Kevlar outer layer, an inner Teflon liner, and a tubular Nylon sock between the ballute and the Teflon liner. During bag strip, the Nylon sock slides against the Teflon liner and inverts, allowing the ballute to deploy from its bag with minimal friction. Unlike a supersonic parachute, the deployment bag is not retained by the ballute after deployment since the risk and consequence of bag recontact are significantly smaller than for a parachute system. The deployment bag closes with the IA protruding out of the pack mouth and a significant portion of the riser is packed into the bag in an annular fashion around the IA. A series of three break ties of varying strength are employed to open the bag mouth in stages after mortar fire. The mortar event caused pack compression due to the rapid acceleration imparted by the mortar. This subsequently resulted in a pack re-expansion while in flight and a tendency to eject the riser from the bag if the bag mouth were completely open, resulting in a disorganized and tangled riser during deployment. The staged bag mouth opening causes most of the pack mouth remained closed until after the pack re-expansion, preventing riser dump.

A flight-like ballute pack is shown in Figure 7 along side the mortar gas generator and Inflation Aid for scale.

Figure 7: Packed ballute next to the mortar gas generator and Inflation Aid.

E. PDD System Mass

A mass breakdown of the flight PDD system is given below in Table 1.

Table 1: PDD softgood mass breakdown.

Item	**Mass (kg)**
Ballute w/ IA Interface H/W	11.1
Inflation Aid	2.19
Riser w/ Kevlar Barrier	1.91
Deployment Bag	0.272
Bag Mouth Cord and Threads	0.193
Ballute Assembly	**15.7**
Triple Bridle w/ Lazy Leg	1.04
Triple Bridle and Confluence Insulation	2.23
Confluence Link	0.105
PDD Deployed Mass	**19.0**

III. Mortar System Description

The mortar system consists of a 27 cm inner diameter aluminum mortar tube, a 4 cm tall aluminum sabot, and a pyrotechnic gas generator utilizing 60 g of black powder. The mortar system accelerates the ballute pack at nearly 600 g's and imparts a nominal impulse of 1080 N-s to the ballute pack. This subsequently results in a nominal reaction load of approximately 23,000 lb and a muzzle velocity of approximately 195 ft/s. Figure 8 illustrates the mortar system with the ballute pack installed. The ballute is installed into the mortar with the IA towards the sabot, thus it was not possible to attach the sabot to the ballute deployment bag as is occasionally done with mortar-deployed parachutes. As such, a Kevlar sabot capture net (not shown in Figure 8) was used to prevent possible contact between the sabot and the ballute. To ensure that the sabot and IA did not damage each other upon mortar fire, a 7.6 cm tall annular wooden spacer was used to transfer the mortar force from the sabot into the ballute and around the Inflation Aid. A 1.3 cm tall crushable honeycomb disc was inserted between the IA and sabot to further attenuate any contact between

the IA and the sabot. The ballute is retained in the mortar tube by a series of pack retention tabs and a single turn of 300 lb Kevlar cord. The force of the mortar pressure is sufficient to break the retention cord and allow the bag to escape.

The mortar tube also features a set of electrical strip heaters and thermal sensors. These heaters are used to heat up to ballute pack and IA to ensure that the IA has sufficient available enthalpy to completely vaporize upon activation (see Section IV.D). The temperature sensors measure the mortar tube temperature both on the ground and in flight.

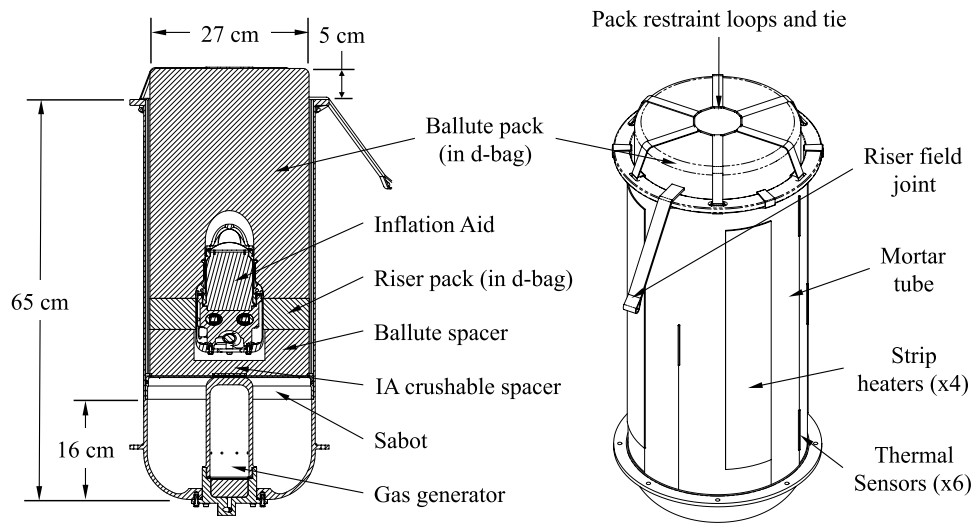

Figure 8: PDD mortar assembly.

The mass breakdown of the mortar system is given below in Table 2, including the total mass ejected by the mortar.

Table 2: Mortar system mass breakdown.

Item	**Mass (kg)**
Ballute Assembly	15.7
Sabot Capture Net	0.315
Sabot	0.718
Sabot Spacer Assembly	1.36
Total Ejected Mass	**18.1**
Mortar Tube	7.0
Heater System	0.879
Gas Generator	4.02
Mortar System Assembly	**29.9**

IV. PDD Pre-Flight Testing and Analyses

The PDD subsystem was subjected to an extensive verification and validation (V&V) test program prior to flight, including subsonic wind tunnel testing, mortar testing, rigging deployment testing, and inflation aid testing. The ballute was never flown at supersonic conditions (sub-scale or full-scale) to obtain aerodynamic data, was not flown in a relevant dynamic pressure to qualify its structural integrity, and it's inflation process was never tested in relevant supersonic flow and low-density conditions prior to flight. Schedule and funding precluded the ability to test these things, but they were each analyzed extensively to buy down the risk of not being able to "test-as-you-fly."

A. Preliminary Wind Tunnel Testing

The ballute was tested in the National Full-scale Aerodynamics Complex (NFAC) 80- by 120-foot Wind Tunnel, located at the NASA Ames Research Center, as part of testing that was performed on sub-scale LDSD parachute designs.[7] The ballute tested was a prototype 4.2 m diameter ballute fabricated of Nylon that was used to get initial drag estimates, qualitative inflation characteristics, and assess inlet height consequences. The ballute exhibited an unusually high drag coefficient ($C_D > 1.0$) in this test that did not correlate well with any existing subsonic drag data for this type of device, thus these data are not presented in detail. No effort was made to structurally qualify the ballute during this test since it was neither the flight design nor the flight material. The testing did show that inlets that were 6 in tall resulted in some light flutter in flight; 4 in tall inlets did not appear to exhibit this behavior. The ballute appeared to retain good pressurization with the 6 in tall inlets where there appeared to be some minor wrinkling with 4 in tall inlets. The ballute was inflated in the wind tunnel using only the ram-air inlets (the inflation aid was not designed yet, and thus was not present). Both the flush and tall inlets did not appear to excessively flutter during inflation and appeared to remain open throughout the inflation process. After this test, 6 in tall inlets were adopted into the design (along with additional structural cords to prevent flutter). Inflation and flight of the ballute in the wind tunnel are shown in Figure 9.

(a) Ballute start of inflation.

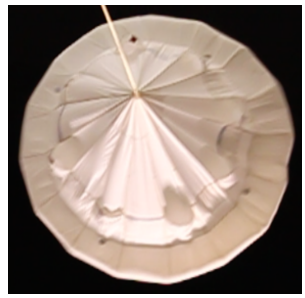

(b) Ballute mid-inflation.

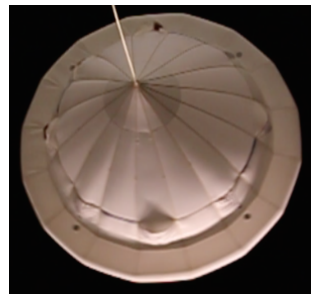

(c) Ballute inflation complete.

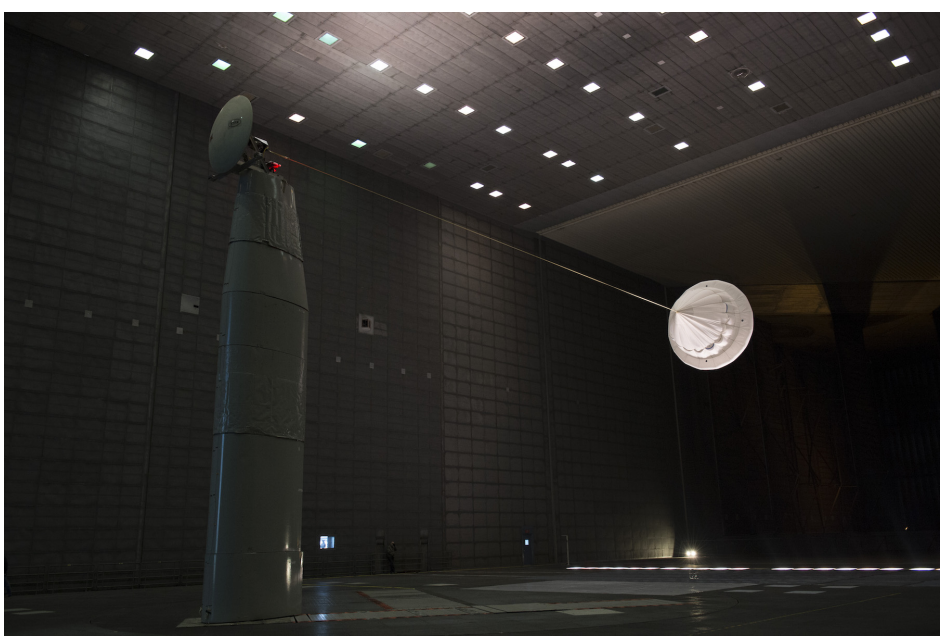

(d) Ballute steady state flight.

Figure 9: Ballute inflation (sans inflation aid) and flight in the NFAC wind tunnel.

B. Pneumatic Mortar Testing

To V&V aspects of the ballute packing method, deployment process, bag strip, and IA activation, the ballute was ejected from a pneumatic mortar at muzzle velocities relevant to the predicted performance of the pyrotechnic mortar. Pneumatic mortar tests were conducted by Pioneer Aerospace at their test facility near South Windsor, CT. The pneumatic mortar setup is shown in Figure 10a. Initial pneumatic mortar tests demonstrated difficulty in sufficiently stripping off of the deployment bag from the ballute, which resulted in the addition of a Nylon tube to the deployment bag (see Section II) to decrease friction. To verify that the IA activated properly and at the appropriate time during bag strip, the redundant IA pyrotechnic charges were redirected to eject colored chalk outside of the IA instead of methanol into the ballute. A set of cameras were lofted approximately 42 m into the air using a weather balloon to capture the bag strip and IA actuation events, shown in Figure 10b. The pneumatic mortar tests could not verify the design of the ballute spacer and IA crushable spacer, however, as the pneumatic system could provide the correct impulse, but could not match the extreme instantaneous force applied by a pyrotechnic mortar.

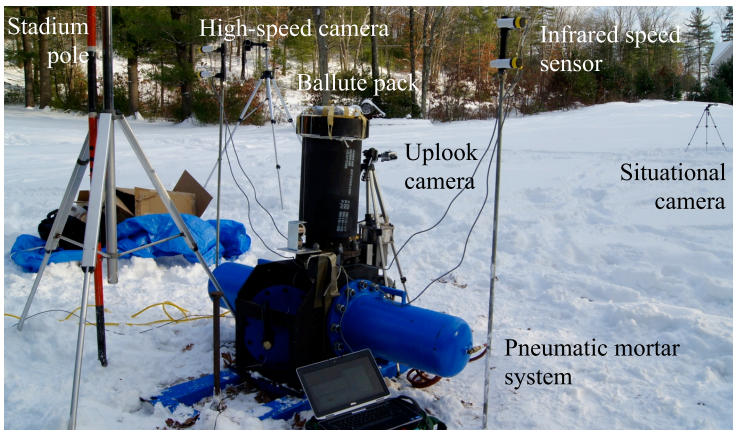

(a) Pneumatic mortar setup.

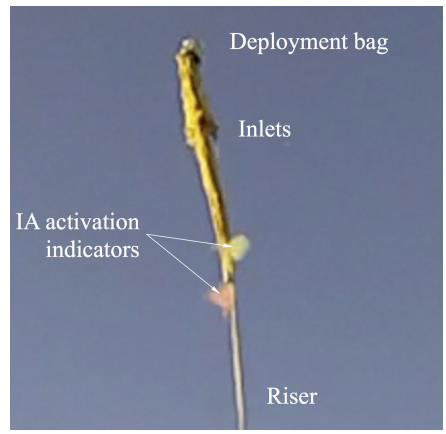

(b) Ballute bag strip and IA activation.

Figure 10: Pneumatic mortar system and test result.

C. Pyrotechnic Mortar Testing

The pyrotechnic mortar system was developed and tested by Systima Technologies in Kirkland, WA. Several firings of the pyrotechnic mortar system were required to properly V&V the mortar performance, the ballute and IA spacer designs, and the sabot capture net strength. In order to obtain good measurements of the mortar performance at altitude, the ullage inside the mortar tube was purged with pure nitrogen to remove the oxygen in between the GG and the sabot. At the 50 km altitude at which the mortar is to function, there is very little oxygen present and the presence of oxygen in the ground-based test can increase GG performance through secondary combustion.

Ballute dunnage pack firings were performed indoors to quantity the mortar pressure, muzzle velocity, reaction loads, and total impulse of the mortar system. These indoor firings did not deploy the ballute or riser, but were crucial in the design iteration of the spacers to ensure that loads were being transmitted appropriately to the ballute back and that the IA and sabot were not being damaged during the mortar fire event. Additionally, these firings demonstrated the need to increase the strength of the sabot capture net to withstand the catch force of the sabot and the spacers.

Outdoor mortar tests were conducted to V&V the ballute pack mouth closure and confirm the ballute bag strip and IA activation witnessed during pneumatic mortar testing. The mortar was fired at a 45° angle over a line suspended by two man-lifts. The purpose of this setup was to catch the ballute by its riser after bag strip to prevent the IA and ballute from hitting the concrete at a high velocity. The mortar fire event during an outdoor test is shown in Figure 11a with the 2nd stage of the bag mouth release occurring in Figure 11b.

Overall, the mortar test program resulted in verification of reliable mortar performance (muzzle velocity and impulse) within a few percent of the values stated in Section III and pre-flight qualification of every part

of the ballute deployment from mortar spacer functionality to organized riser strip out to IA activation.

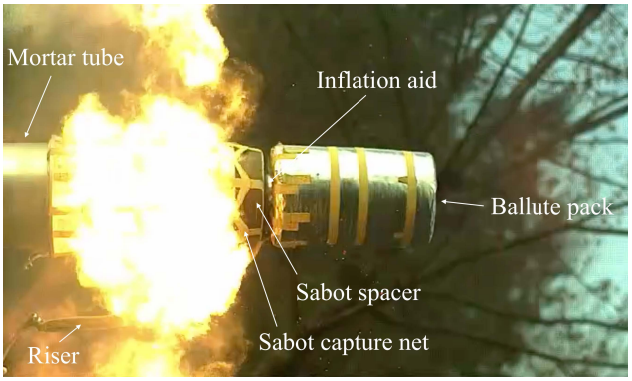

(a) Mortar fire event showing sabot and spacer capture and ballute compression.

(b) 2nd stage bag mouth release after approximately 2.4 m of riser was deployed.

Figure 11: Pyrotechnic mortar testing.

D. Inflation Aid Testing

The IA underwent an extensive V&V program prior to being implemented on the flight TV. A prototype IA was tested in a vacuum chamber to verify the pyrotechnic actuation concept, confirm methanol ejection and vaporization, and validate methanol vaporization analyses. The IA was tested both without the ballute and with the ballute present in the vacuum chamber, as shown in Figure 12. In this test, the chamber pressure was measured and the ballute was instrumented to obtain the differential pressure between the inside and outside of the ballute.

The data from these vacuum chamber tests indicated that there was insufficient energy available to reliably vaporize 100% of the methanol contained within the IA. In order to ensure that the IA performance requirement was achieved, the IA had to be heated to approximately 40°C in order to increase the thermal energy available for methanol vaporization. Details of the vacuum chamber tests that lead to this results are provide by Thompson et al.[6]

In order to get the IA to the desired temperature in flight, the mortar assembly was wrapped in 1 in thick alumina insulation and heated prior to flight using the strip heaters on the mortar tube shown in Figure 8. The heaters could not operated during flight due to battery power limitations on the TV and heater power had to be disconnected anywhere from 12 to 20 hours prior to the estimated PDD mortar fire time due to launch constraints. Since the IA could not be heated directly and could not be instrumented in the actual flight system, a flight system mockup was instrumented and ground tested in order to characterize the thermal behavior of the insulated PDD mortar assembly. For this test, the PDD was heated for approximately 36

(a) Methanol ejection and vaporization.

(b) Prototype ballute inflation.

Figure 12: Inflation Aid prototype tests in a vacuum chamber at a 50 km altitude equivalent pressure.

hours at a set temperature of 86°C. The long heat duration was required for the heat to soak through the ballute pack and heat the IA to a temperature of 80°C. When the IA reached a temperature of 80°C, the heater power was disconnected and the system as allowed to cool. As shown in Figure 13, the insulation provided by the alumina wrap and the Kevlar ballute pack kept the IA above the targeted 40°C temperature for approximately 18 hours, which was deemed sufficient for the first flight.

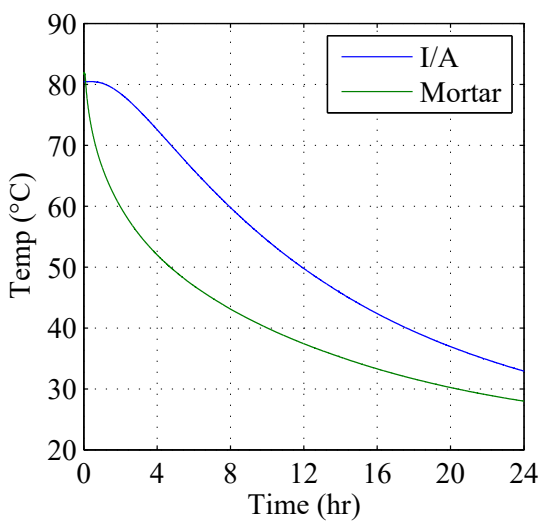

Figure 13: PDD mortar tube and IA temperature as a function of time with flight insulation present and heater power off.

E. Aerodynamic and Aerothermal Analyses

A preliminary aerodynamic database for the ballute was constructed based on historical test data of similar devices, as shown in Figure 14a. Extensive computational fluid dynamics (CFD) simulations were conducted on the ballute in the TV wake, as shown in Figure 14b, to verify these aerodynamics and to calculate worst-case drag performance in the vehicle wake. These simulations were also used to help determine the position and efficiency of the ballute inlets.[8] Simulations were also performed post-fight to correlate the simulation parameters to observed flight behavior. These pre- and post-flight aerodynamic results are discussed in detail by Muppidi et al.[9]

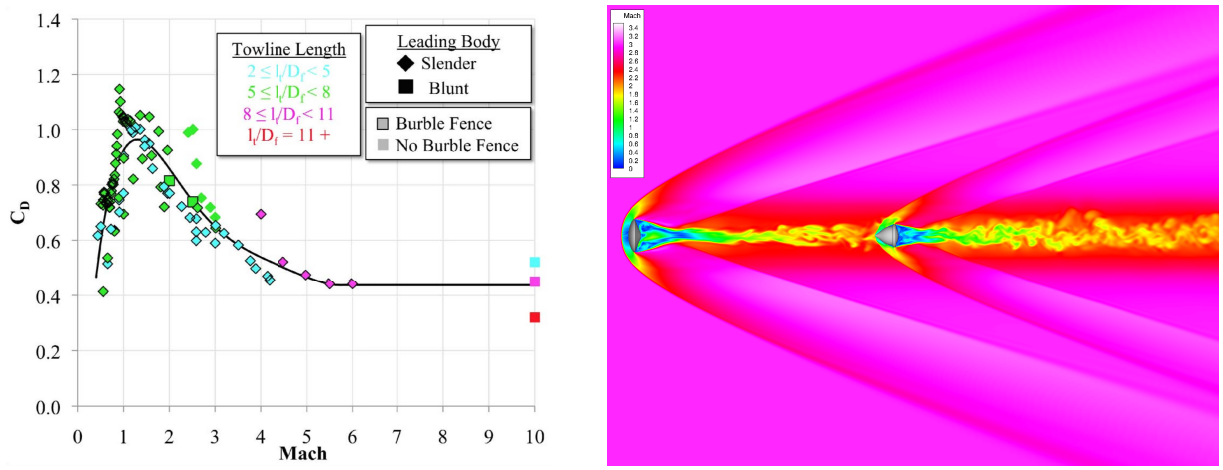

(a) Preliminary ballute aerodynamic model.[10]

(b) Example of ballute CFD result.

Figure 14: Ballute aerodynamics modeling and simulation.

CFD simulations were also used to help determine the aerothermodynamic environment of the ballute in flight. The CFD simulations were used to develop aerothermal indicators, which identified hot spots on the ballute surface and how hot these spots were relative to other areas on the ballute. These CFD results were used in conjunction with trajectory dispersions to determine the heat flux into the ballute and calculate the range of possible temperatures that the ballute may experience in flight. Figure 15 shows the predicted hot regions of the ballute (shown in red) and the 90% high fabric temperature of the ballute in a couple key areas for a Mach 3 deployment. In general, ballute temperatures were not expected to exceed 290C and structural margins were still positive with thermal knockdown factors consistent with these temperatures.

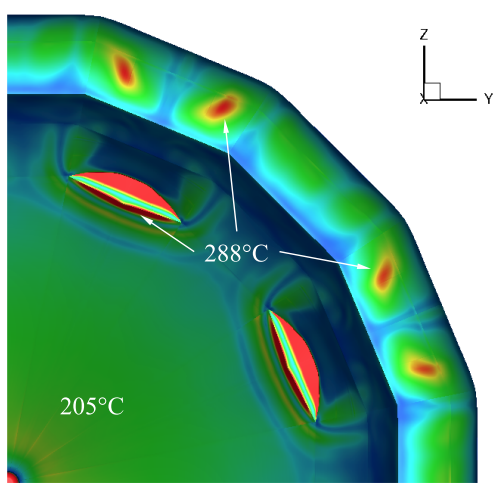

Figure 15: Aerothermal hot spots are indicated in red on the ballute with the 90% high fabric temperatures in key areas shown.

F. Structural Analyses

The ballute structure was analyzed using the finite element analysis (FEA) code LS-DYNA. The initial ballute shape was generated assuming a Newtonian pressure distribution.[11] The shape was then iterated with more accurate windward and leeward pressure coefficient distributions from CFD analyses until a final shape was converged upon. The internal pressure of the ballute was assumed to be equal to the dynamic pressure within the wake core of the vehicle and the external pressure was set to generate the design drag

load of 1680 lb. Under these loading conditions, the ballute exhibited positive structural margins across all elements. Structural analysis of the ballute is detailed by Grychanyuk et al.[12]

V. Flight Performance

The first LDSD Supersonic Flight Dynamics Test (SFDT) occurred on June 28th, 2014 in Kauai, HI. The overall SFDT concept of operations is shown in Figure 16. Trajectory reconstruction indicated that PDD mortar fire at a Mach number of 2.73, a geodetic altitude of 50 km, and a dynamic pressure of 429 Pa. The ballute flew for 5 seconds until the bridles were cut and the ballute extracted the parachute.

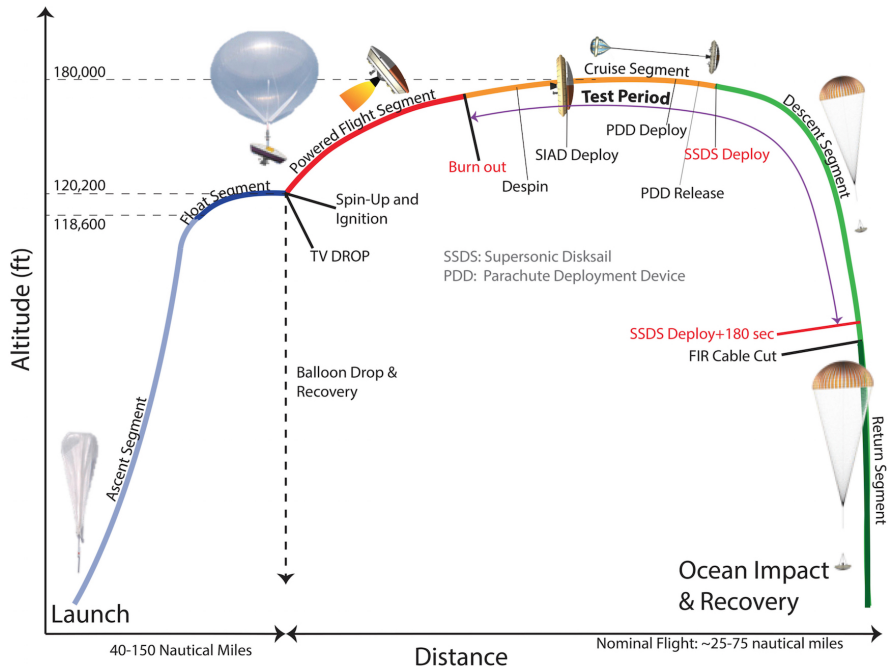

Figure 16: LDSD SFDT concept of operations.

A. Instrumentation

Each of the three PDD bridle fittings were equipped with a 3000 lb capability load pin to directly measure the drag load of the ballute with a 4.5% uncertainty at a data rate of 1 kHz. An inertial measurement unit (IMU) was also present to measure vehicle translation and rotational accelerations. Additionally, there was a high-speed camera recording at 135 frames per second (fps), a high-resolution camera recording at 16 fps, and several high-definition situational cameras recording at 30 fps. These data, in conjunction with the reconstructed TV trajectory, enabled relatively accurate determination of the ballute's drag performance, the IA performance, and a time history of the ballute's position relative to both the vehicle and the relative wind. Note that the ballute itself was not instrumented to obtain internal pressure measurements.

B. Deployment

The ballute mortar was initiated at 161.58 seconds after the TV was dropped from the balloon and the ballute takes approximately 0.014 seconds to exit the mortar tube, thus the ballute should have achieved muzzle velocity at approximately 161.59 seconds. Line stretch occurred when the ballute pack reached a distance of 41.7 m from the aft side of the TV, based on the dimensions in Figure 6. Line stretch occurred at a time of 162.34 seconds, based on the load spike measured by the PDD bridle pin loads, resulting in a 0.75 second free flight time between mortar ejection and line stretch (Δt_{ls}). The IMU measured a nearly constant vehicle deceleration of 11 m/s^2 during these 0.75 seconds. Using Equation 1, the muzzle velocity (V_0) was estimated to be 60 m/s, which agrees well with the 59 m/s muzzle velocity measured during ground

based mortar testing. The line stretch velocity of the ballute pack can be similarly estimated using Equation 2, which results in a pack velocity of 52 m/s.

$$V_0 = \frac{x_{ls}}{\Delta t_{ls}} - \frac{a_{TV}\Delta t_{ls}}{2} \tag{1}$$

$$V_{ls} = a_{TV}\Delta t_{ls} + V_0 \tag{2}$$

Between mortar fire and line stretch, the PDD bridles exhibited a significant amount of dynamic motion. The bridles deployed from their stowed state and stood up within approximately 0.2 seconds of mortar fire. Due to the relatively high momentum of the bridles during standup, they recoil and partially collapse back onto the aft deck of the vehicle immediately after standup. Bridle leg 1 temporarily collapses into the conical section of the vehicle aft deck and bridle leg 2 collapses near a spin motor, as shown in Figure 17. It is also believed that the bridles came into contact with the main motor nozzle during this time. Despite these dynamics, the bridles did not snag on any vehicle item during deployment and did not damage any of the vehicle hardware or instrumentation. Bridle dynamics such as this was expected based on bridle extraction testing,[?] although bridle collapse of this extent was not witnessed during ground-based testing. Snag shields have been strategically implemented on subsequent SFDT flights to reduce the risk of PDD bridle snags during this dynamic period.

(a) Bridle leg 1.

(b) Bridle leg 2.

Figure 17: Momentary slack observed in bridle legs 1 and 2 with slack around the spin motor being of particular concern due to the potential for snag.

The total snatch force at line stretch was measured to be 4330 lb at the vehicle load pins, with almost 65% of this force being transmitted through bridle leg 1 due to the orientation of the TV. This high line stretch load is largely attributed to the sudden snatch of the relatively massive IA device (approximately 2.2 kg). This snatch force also caused a significant amount of recoil, which is visible in Figure 18. The recoil and associated re-snatch of the slack in the riser and bridles caused large magnitude oscillations in the measured bridle loads, shown in Figure 19.

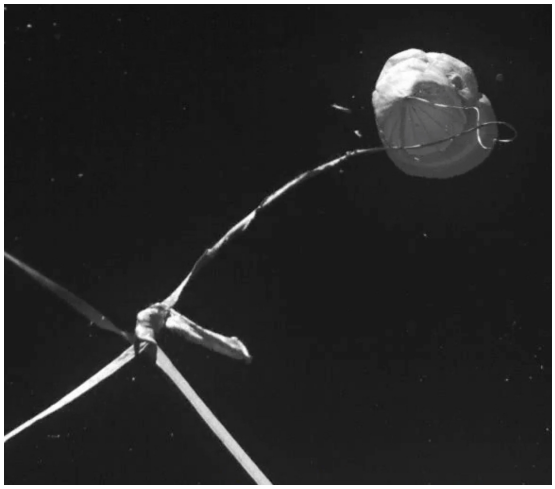

Figure 18: Riser slack apparent approximately 0.2 seconds after line stretch due to recoil.

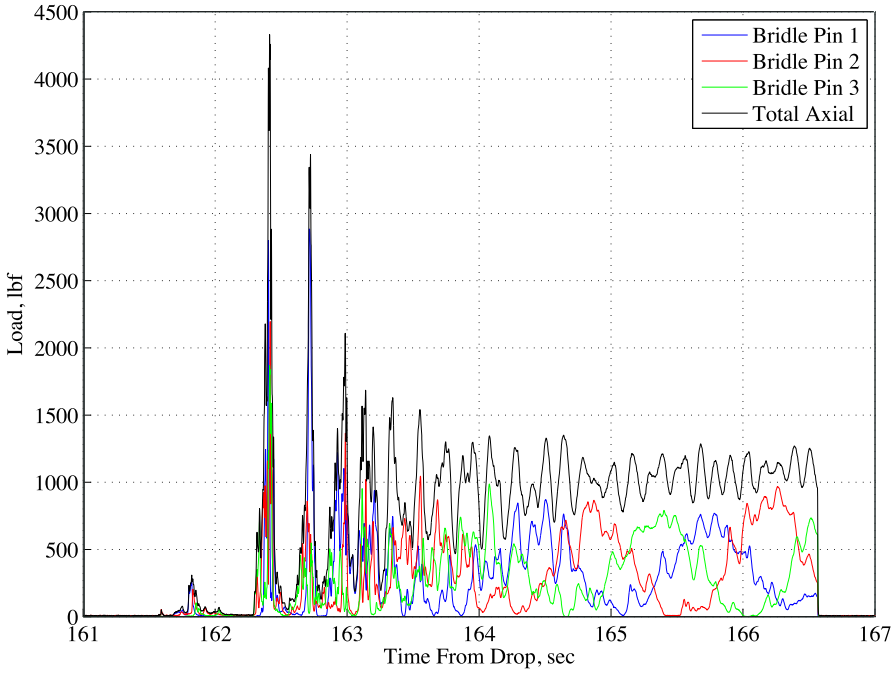

Figure 19: Ballute load time history for each load pin and total.

C. Inflation

The ballute inflation process, from line stretch to full inflation, is shown in Figure 20. After mortar fire, the ballute gradually rotated into a near perpendicular orientation relative to the freestream. Similar pack rotation was observed during ground-based mortar testing as well. The magnitude of the ballute pack's rotation was assumed to be due to the center of mass of the pack being located towards the riser end of the pack due to the presence of the IA. Mortar-fired parachute packs typically exhibit some small rotation, but their pack center of mass is generally located near the center of the pack.

It should be noted that the disc visible in the first five images in Figure 20 is a piece of the softgood TPS covering the mortar tube and is not the sabot, which was captured

In Figure 20, the IA appears to have triggered just prior to 162.44 s, as evidenced by the sudden inflation and lobing at the nose of the ballute without presentation of the ballute inlets. Pressure measurements inside the ballute were not obtained during inflation or flight; however, the pressure supplied by the IA

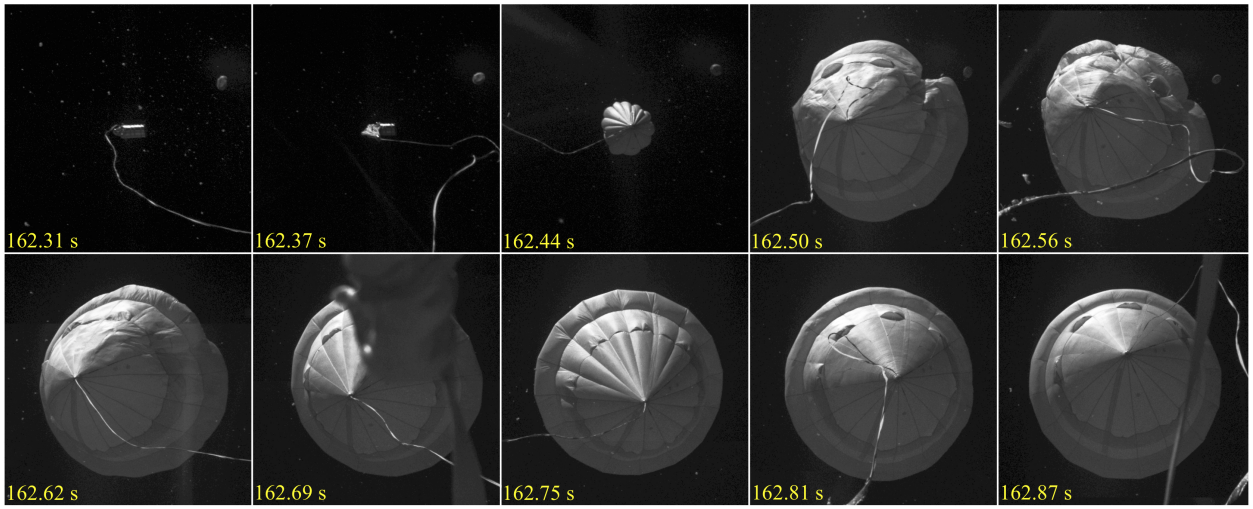

Figure 20: Ballute inflation sequence with the reconstructed time from drop in each image. Ballute inflation occurred in approximately 0.56 seconds.

can be estimated based on pre-flight thermal characterization of the IA. For this flight, launch operations and weather patterns permitted mortar fire to occur only 12 hours after the PDD heater was disconnected. According to Figure 13, the IA temperature would have been approximately 50°C at 12 hours. Using the equations provided in Thompson et al.,[6] the IA would have provided approximately 99% of the ballute internal pressure expected at a deployment Mach number of 2.73 and an altitude of 50 km.

The inflation sequence in Figure 20 also indicates that the ballute did not exhibit an inflation process similar to that shown in Figure 9. It appears that the pressure supplied by the IA prevented concavity in the ballute gores during inflation, which effectively disallowed the flush inlets to open and ingest air during inflation. From these data, it is difficult to determine how fast or how effectual the flush inlets would have been in the absence of a pre-inflation system such as the IA.

D. Aerodynamic Behavior

The steady-state axial force generated by the ballute during its last three seconds of flight was just over 1000 lb, resulting in a drag coefficient (C_D) of approximately 0.6, as shown in Figure 21a. The mean drag coefficient exhibited in flight appears to agree well with the high bound of the ballute aerodynamics model used for pre-flight vehicle trajectory and performance analyses, as shown in Figure 21b. Given these drag coefficient data and the drag coefficient of the TV (with the SIAD deployed) just prior to PDD deployment, the ballute increased the total drag area of the flight system by approxiamtely 21%.

To better understand why the ballute drag coefficient was on the upper end of the pre-flight model and where the ballute flew relative to the TV, the ballute's three-dimensional position was reconstructed using a photogrammetric analysis of the high-speed camera data, a known transformation between the camera image frame and the vehicle frame, and a 3D engineering model of the inflated ballute. This analysis method is briefly described by Muppidi et al.[9] Combining these results with the reconstructed vehicle dynamics and wind-relative attitude, a time history of the ballute's flight relative to the wind vector could be obtained.

Figure 22 is a diagram of the reconstructed position of the behind the vehicle at four instants in time. A plane aligned with the middle of the ballute burble fence is illustrated with a black circle on the left plot and a black plane on the right two plot. The red dashed lines represent the TV's wake and illustrates the vehicle's angle of attack and sideslip angle. The plots in Figure 22 help show that the ballute flew within the wake of the TV, but did *not* fly in the center of the TV wake, where it would experience the greatest dynamic pressure deficit. Note that the CFD-generated aerodynamics *did* assume that the ballute flew in the center of the vehicle wake in order to generate a more conservative ballute drag estimate (see Section IV.E). The ballute tended to fly near the edge of the wake, where the wake deficit was significantly less, which subsequently resulted in a higher ballute drag performance. The reason for this behavior was that the TV was nutating, as is indicated by the counter-clockwise motion of the wake around the TV, and the

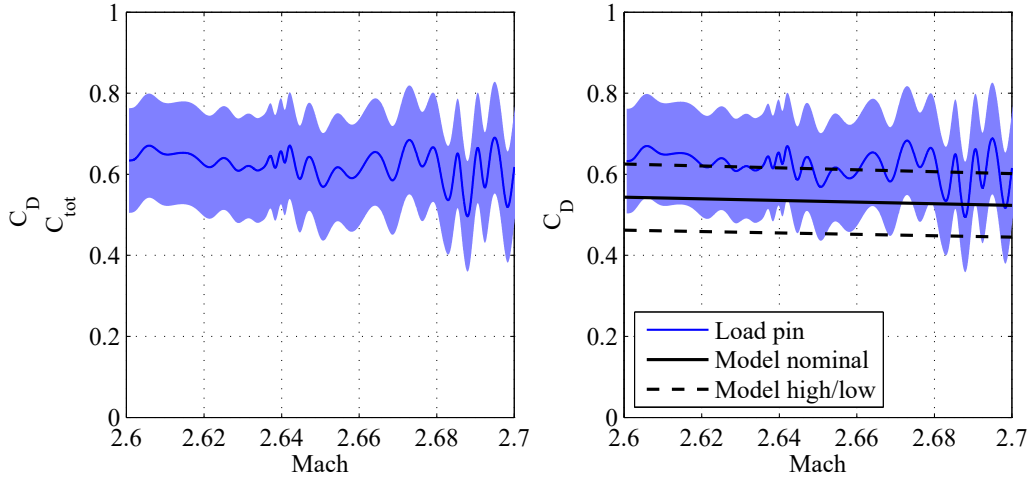

(a) Ballute C_D time history (unfiltered).

(b) Ballute C_D (5 Hz filtered) compared to pre-test model values.

Figure 21: Ballute drag coefficient calculated from the load pin data according Muppidi et al.:[9] solid line shows nominal data and the shadowed region shows the 3σ confidence bounds.

Figure 87: Ballute total force coefficient (C_{tot}) reconstructed from load pin measurements filtered at 5 Hz, and pre-flight predicted ballute drag coefficient (C_D) as a function of wind-relative Mach number for the last 3 seconds of ballute flight. The shaded regions indicate the 3-σ confidence interval on C_{tot}, and the dashed lines indicate the high and low bounds in the preflight C_D prediction.

The increased pitch and yaw axis rotation rates are reflected in the measured vehicle accelerations (Figure 93). In Figure 93, a spike in the y and y axis accelerations is evident at mortar fire. The subsequent lower-frequency oscillations in the acceleration are correspond to the vehicle's rotational motion, while the higher frequency oscillations arise from the oscillations in the ballute force evident in Figure 85.

The time history of the vehicle velocities are presented in Figure 94. The oscillation in the y

a f the

d

(14)

t lt of

b g the

f ately

w leslip

a gle of

i ttack

n ional

o the

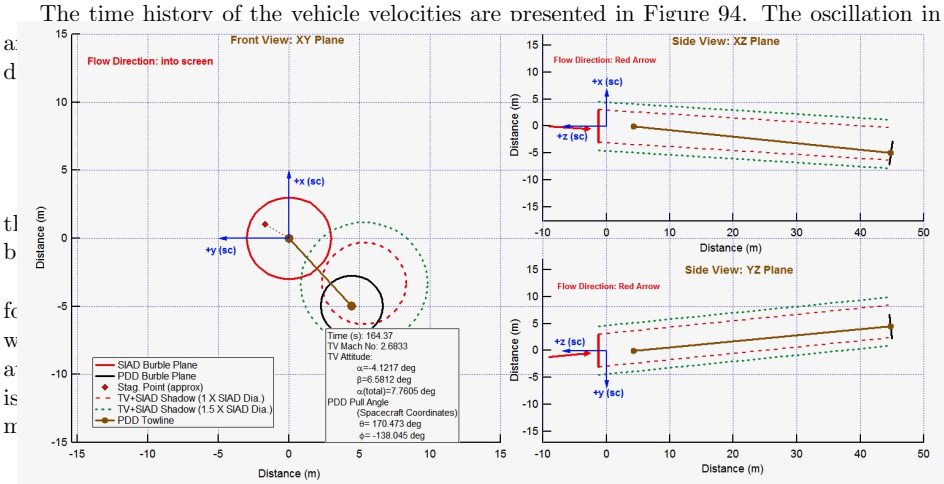

(a) 164.37 s

Pre-Decisional for Internal Discussion Purposes Only
The technical data in this document is controlled under the U.S. Export Regulations;
release to foreign persons may require an export authorization.

Figure 22: Diagrams showing the reconstructed ballute position relative to the TV wake during the SFDT-1 flight at four instances in time. These data illustrate that the ballute flew near the edge of the TV wake, not in the wake core, and thus exhibited higher than expected drag performance. (Continued on next page)

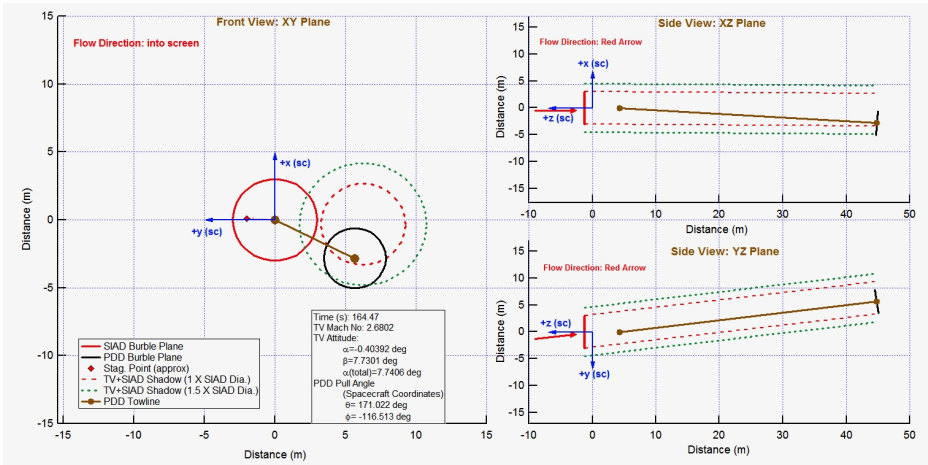

(b) 164.47 s

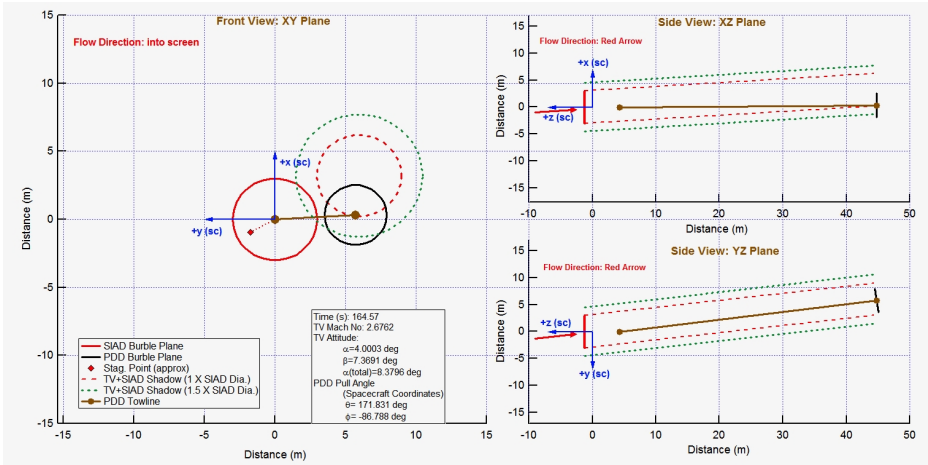

(c) 164.57 s

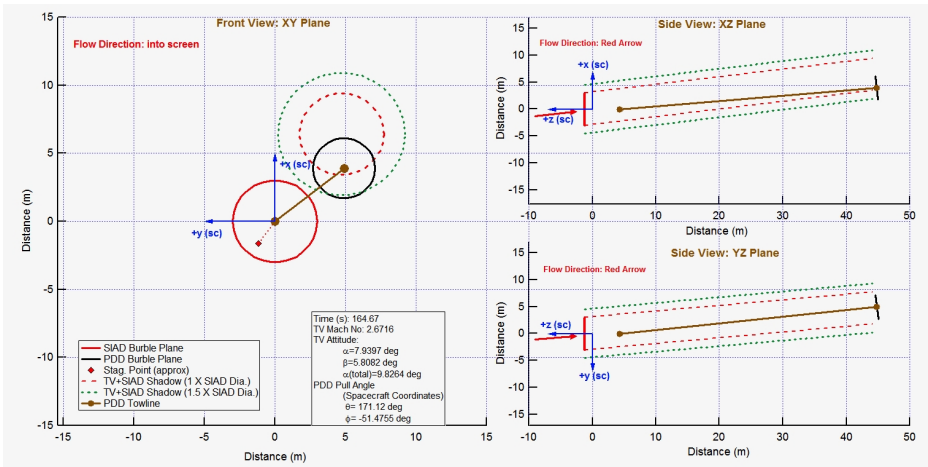

(d) 164.67 s

Figure 22: Diagrams showing the reconstructed ballute position relative to the TV wake during the SFDT-1 flight at four instances in time. These data illustrate that the ballute flew near the edge of the TV wake, not in the wake core, and thus exhibited higher than expected drag performance. (Continued from previous page)

ballute was "pushed" to follow this nutation as it could not escape the steep pressure gradient near the edge of the wake.

VI. Recovery and Inspection

Post-flight recovery of the ballute was not expected due to the inability to include any tracking devices on the ballute, the uncertain trajectory after separation, and timeliness required to retrieve the data from the TV. However, purely by coincidence, the recovery boats ran across the ballute while en route to recover the TV and were able to pull it aboard quickly. Images of the ballute recovery are shown in Figure 23. The ballute had ingested a significant amount of water, so the recovery divers had to cut several holes in the device to bleed the water from the ballute as it was being pulled onto the boat.

(a) Ballute afloat in the ocean.

(b) Pulling the ballute onboard; holes had to be cut to relieve the water.

Figure 23: Images of the recovery of the ballute.

Overall, inspection of the ballute indicated that it was in remarkable condition during and after flight. Particularly interesting inspection notes are as follows:

- There was no damage or discoloration to any part of the ballute or IA to indicate aerothermal conditions exceed the capability of the materials. Even the inlet cords, the items with the smallest radii on the ballute, did not exhibit any aerothermal or structural damage. Some discoloration and damage was present due scraping across the edge of the boat as it was being pulled aboard, as shown in Fig 24.
- Both of the redundant pyrotechnic devices in the IA fired and the rupture disk was open, indicating that the IA operated nominally.
- The bridle and riser webbing did not exhibit any damage due to overload or contact with the main motor nozzle, although there was some damage to the riser due to recovery, as shown in Figure 24b
- The riser exhibited a few minor black dots on the surface of its thermal protection layer, indicating that the riser likely encounter some hot particles from the rocket motor. There was not evidence that hot material penetrated all the way though the thermal protection.
- There was no discoloration or damage that could be associated with an excessively hot thermal environment, indicating that the thermal protection layers around the bridles were sufficient for the main motor burn environment. Additionally, it indicates that spin motor plume shields around the PDD bridles were effective.
- There was a small area of Kevlar comb out at one seam on the burble fence, as shown in Figure 24c. Since this damage does not appear anywhere else on the ballute and the comb out is oriented on the same side of the ballute as the cuts made by the recovery divers, it is believed that this comb out

occurred during recovery, likely due to the excessive weight of the water in the burble fence while it was being pulled aboard the boat.

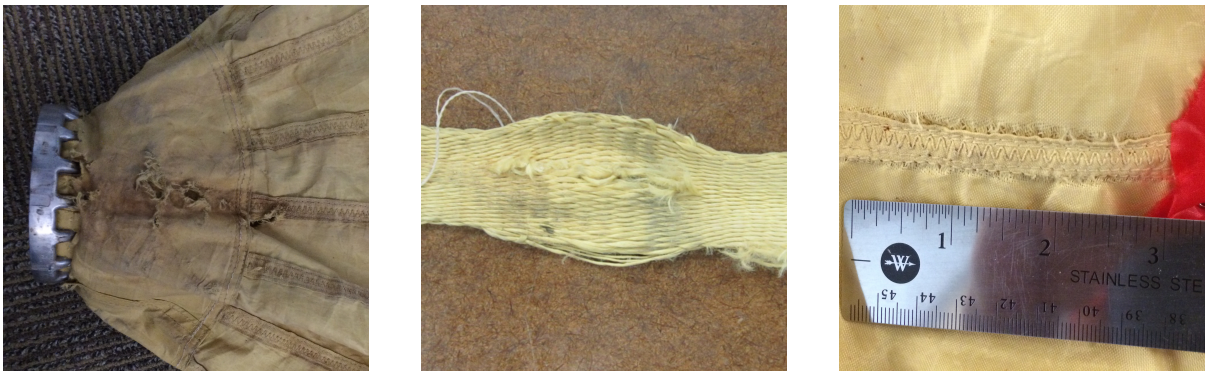

(a) Abrasion damage near IA. (b) Riser damage due to recovery. (c) Comb out at burble fence.

Figure 24: Damaged areas of the ballute, all attributed to recovery activities.

VII. Summary

The LDSD Project developed a 4.4 m diameter supersonic ram-air ballute as a pilot device to extract its supersonic parachute. The ballute was fabricated from a 60x60 weave of silicon-impregnated Kevlar for strength, thermal resilience, minimum permeability. The ballute featured eight 6 in tall ram-air inlets that were used to maintain pressure inside the envelope during its 5-second flight as well as eight flush-mounted inlets that were used to assist ballute inflation. The ballute was analyzed in the TV wake core using CFD to develop a pre-flight aerodynamic database, which conservatively estimated the nominal ballute drag coefficient to be around 0.5 for a Mach 2.7 deployment. Structural and aerothermal analyses were conducted and showed that the ballute could potentially experience temperatures as high as 288°C, but also showed that structural margins were sufficient for the ballute to withstand the FLL of 1680 lb with the appropriate thermal knockdown factors.

One of the primary efforts associated with the ballute was the development of a mechanically actuated pyrotechnic inflation system utilizing liquid methanol. This type of Inflation Aid was selected to due to similarity to previous gas generators used in ballute devices back in the 1960's. The IA attached to the front of the ballute and served a dual purpose as the main interface to the riser. The IA underwent a series of functionality tests in vacuum to ensure that the gas generation process was well understood. The IA was then tested in pneumatic and pyrotechnic mortar tests to ensure that the lanyard actuation mechanism performed as designed.

The ballute was successfully flown in June 2014 and successfully extracted the supersonic parachute as designed. In-situ load measurements indicated that the ballute performed better than pre-flight predictions. Reconstruction of the ballute position relative to the TV indicated that the ballute tended to stay within the wake of the vehicle, but near the edge of the wake where dynamic pressure loss was less than estimated in pre-flight analyses. Recovery of the ballute showed that the structure was not compromised due to flight loads or due to excessive aerothermodynamic heating.

The flight of the LDSD ballute represents the largest ballute ever successfully deployed and flown at a Mach number as high as 2.7. Previously, the Goodyear Aerospace Corporation attempted to deploy a 5.5 m diameter ram-air ballute at a Mach number of 3.15 in 1969 under contract to NASA Langley Research Center, but failed to inflate.[4] This particular ballute did not utilize a pre-inflation system, thus the failure of the ballute was largely attributed to slow inflation (due to relying solely on the inlets) and the subsequent damage to the ram-air inlets.

Acknowledgements

The Low Density Supersonic Decelerator project is directed by the Jet Propulsion Laboratory, California Institute of Technology, under a contract with the National Aeronautics and Space Administration. The authors would like to acknowledge the exceptional work performed by personnel at the Pioneer Aerospace Corporation, Systima Technologies Inc., and NASA Ames Research Center in the successful development of a large supersonic ballute and its deployment system under significant schedule pressure and system constraints.

References

[1]Adams, D., "Mortar Deployment Extensibility for the Low Density Supersonic Decelerator Parachute," *IEEE Aerospace Conference,* IEEAC Paper 2659, Big Sky, MT, 2014.

[2]Gallon, J., Clark, I., and Witkowski, A., "Parachute Decelerator System Performance During the Low Density Supersonic Decelerator Program?s First Supersonic Flight Dynamics Test," *23rd AIAA Aerodynamic Decelerator Systems Technology Conference and Seminar,* AIAA 2015-XXXX, Daytona Beach, FL, March 2015.

[3]Woodruff, P., Yanaros, C., Witkowski, A., and Tanner, C., "LDSD Supersonic Ballute Design and Packing," *23rd AIAA Aerodynamic Decelerator Systems Technology Conference and Seminar,* AIAA 2015-XXXX, Daytona Beach, FL, March 2015.

[4]Bloetscher, F., "Aerodynamic Deployable Decelerator Performance-Evaluation Program, Phase II," Tech. Rep. AFFDL-TR-67-25, Goodyear Aerospace Corporation, Dayton, OH, June 1967.

[5]Mayhue, R. and Eckstrom, C., "Flight-Test Results From Supersonic Deployment of an 18-Foot-Diameter (5.49-Meter) Towed Ballute Decelerator," Tech. Rep. NASA TM X-1773, NASA Langley Research Center, Hampton, VA, May 1969.

[6]Thompson, N., Karp, A., Tanner, C., and Gallon, J., "Pyrotechnically Actuated Gas Generator Utilizing Aqueous Methanol," *23rd AIAA Aerodynamic Decelerator Systems Technology Conference and Seminar,* AIAA 2015-XXXX, Daytona Beach, FL, March 2015.

[7]Tanner, C., Clark, I., Gallon, J., Rivellini, T., and Witkowski, A., "Aerodynamic Characterization of New Parachute Configurations for Low-Density Deceleration," *22nd AIAA Aerodynamic Decelerator Systems Technology Conference and Seminar,* AIAA 2013-1358, Daytona Beach, FL, March 2013.

[8]Muppidi, S., Tang, C., Norman, J. V., Bose, D., Clark, I., and Coatta, D., "Aerodynamic Analysis of Next Generation Supersonic Decelerators," *32nd AIAA Applied Aerodynamics Conference,* AIAA 2014-2990, Reston, VA, June 2014.

[9]Muppidi, S., Norman, J. V., O'Farrell, C., Bose, D., and Clark, I., "Computational Analysis and Post-Flight Validation of Ballute Aerodynamics," *23rd AIAA Aerodynamic Decelerator Systems Technology Conference and Seminar,* AIAA 2015-XXXX, Daytona Beach, FL, March 2015.

[10]Smith, B., Tanner, C., Mahzari, M., Clark, I., and Braun, R., "A Historical Review of Inflatable Aerodynamic Decelerator Technology Development," *IEEE Aerospace Conference,* IEEEAC Paper 1276, Big Sky, MT, March 2010.

[11]Houtz, N., "Optimization of Inflatable Drag Devices by Isotensoid Design," *1st AIAA Annual Meeting,* AIAA 1964-437, Washington D.C., June 1964.

[12]Grychanyuk, V., Kandis, M., Witkowski, A., and Tanner, C., "Stress Analysis of the LDSD Supersonic Ballute," *23rd AIAA Aerodynamic Decelerator Systems Technology Conference and Seminar,* AIAA 2015-XXXX, Daytona Beach, FL, March 2015.